

Research Article

Jose L. Ocaña*, R. Jagdheesh and J.J. García-Ballesteros

Direct generation of superhydrophobic microstructures in metals by UV laser sources in the nanosecond regime

DOI 10.1515/aot-2016-0002

Received January 5, 2016; accepted January 22, 2016; previously published online February 29, 2016

Abstract: The current availability of new advanced fiber and DPSS lasers with characteristic pulse lengths ranging from ns to fs has provided a unique frame in which the development of laser-generated microstructures has been made possible for very diverse kinds of materials and applications. At the same time, the development of the appropriate laser-processing workstations granting the appropriate precision and repeatability of the respective laser interaction processes in line with the characteristic dimension features required in the microstructured samples has definitively consolidated laser surface microstructuring as a reference domain, nowadays, unavoidable for the design and manufacturing of current use microsystem: MEMSs, fluidic devices, advanced sensors, biomedical devices and instruments, etc., are all among the most well-known developments of the micromanufacturing technology. Completing the broad spectrum of applications developed mostly involving the generation of geometrical features on a substrate with specific functional purposes, a relatively new, emerging class of laser-microstructuring techniques is finding an important niche of application in the generation of physically structured surfaces (particularly of metallic materials) with specific contact, friction, and wear functionalities, for whose generation the concurrence of different types of laser sources is being found as an appropriate tool. In this paper, the application of laser sources with emission in the UV and at ns time regime to the surface structuration of metal

surfaces (specifically Al) for the modification of their wettability properties is described as an attractive application basis for the generation of self-cleaning properties of extended functional surfaces. Flat aluminum sheets of thickness 100 μm were laser machined with ultraviolet laser pulses of 30 ns with different laser parameters to optimize the process parameters. The samples produced at the optimum conditions with respect to contact angle measurement were subjected to microstructure and chemical analysis. The wetting properties were evaluated by static contact angle measurements on the laser-patterned surface. The laser-patterned microstructures exhibited superhydrophobicity with a maximum contact angle of 180° for the droplet volumes in the range of 8–12 μl .

Keywords: laser surface structuration; ns lasers; superhydrophobicity.

1 Introduction

In recent years, the generation of functional surfaces emulating natural structures has gained considerable interest due to their potential industrial applications. Among the most sought functional properties, the high degree of water repellence (superhydrophobicity) characteristic of the lotus (*Nelumbo nucifera*) leaf has gained increasing interest for research due its anti-corrosion and low hydrodynamic friction properties [1, 2].

Inspired by these water repellence and self-cleaning properties of the lotus leaf, successful attempts have been made to change the surface wettability of different materials in two main different ways or a combination of both: (a) by modifying the surface chemistry by means of chemical coatings in order to reduce the surface free energy [3]; (b) by surface micromanipulation in order to generate micro/nano dual-scale (hierarchical) surface roughness patterns [4].

Concerning the different methods for the achievement of the referred modification of wetting properties,

*Corresponding author: Jose L. Ocaña, UPM Laser Centre, Universidad Politécnica de Madrid, Ctra. Valencia, km 7.3, 28031 Madrid, Spain, e-mail: jlocana@etsii.upm.es. <http://orcid.org/0000-0001-9263-8404>

R. Jagdheesh and J.J. García-Ballesteros: UPM Laser Centre, Universidad Politécnica de Madrid, 28031 Madrid, Spain

different kinds of techniques like photolithography, nano-casting, extrusion, placement of carbon nanotubes, etc., have been adopted with the common objective of creating a large-scale roughness in a variety of materials. However, these techniques suffer from weaknesses related to the high cost of projection masks and high development times in the different steps involved in creating the desired periodical roughness patterns.

At their turn, ultrafast laser sources can be used to create a variety of micro/nano structures in an open environment in a reliable way. Normally, the superhydrophobic property can be realized through a controlled ablation patterning of the surface and subsequent application of different chemical coatings on the machined area in order to decrease the generally high surface energy of the initially machined surface in a classical ‘two-step’ process.

However, recent studies on laser micromachining have demonstrated their ability to fabricate micro/nanoscale features with very limited distortion to the peripheral area [5, 6], and superhydrophobic effects were reported on ceramics using a single-step (i.e. direct laser ablation) procedure by one of the authors [3].

Considering, on the other hand, that the application of an external coating material onto the laser-structured surface is, in general, undesirable (especially in the case of metallic surfaces) as it manipulates the surface chemistry with resulting limited durability of the superhydrophobic behavior, seeking for the capability of a one-step technique introducing the required modified wettability properties, especially in metallic substrates, seems to be a clear practical need.

Different authors (see, i.e. refs. [7–9]) have investigated thoroughly the application of short and ultrashort laser pulses, predominantly in the IR domain, to the ablation micromachining of different materials, including metals, concluding on the convenient use of lasers with pulses in the ps regime in order to avoid excess of material heat-affected zones and associate thermal effects. However, not much research has been published on the application of lasers with pulses in the ns regime and with emission in the VUV domain to the generation of surface micro/nanostructures. Several authors (see, i.e. refs. [10, 11]) have, nevertheless, published interesting results on the application of ns laser pulses in different types of materials, showing that with the appropriate choice of laser parameters and processing strategies, nanosecond lasers can be used for high-quality micromachining in metals, ceramics, and polymers and that the detailed dependency of the surface quality for different materials and laser parameters is really very complex and deserves a particularized study for each kind of application.

Concerning the concrete field of the transformation of the wettability properties of different metallic surfaces, several interesting studies have been published on the direct applicability of lasers at different fluence levels for the generation of different degrees of hydrophobicity (see, i.e. refs. [12, 13]) and on the use of fs and ns pulses for the generation of multiscale surface features that are conceptually useful from the point of view of the generation of hierarchical surfaces [14–19].

On the basis of these advantageous possibility, the work presented in this paper deals with the use of ns lasers with emission in the UV ($\lambda=355$ nm) to the controlled generation of different kinds of micro/nano features presumably leading to modified wettability properties (high degree of hydrophobicity) in typical metallic materials (Al being used as a representative sample).

Concretely, ns laser pulses were applied on flat substrates of aluminum (Al) to fabricate micropillars, two different geometries such as microchannels and micropillars having been studied with respect to the generation of high static contact angles (SCAs).

2 Experimental

Flat aluminum (Al) sheets, 100 μm thick, and negligible roughness were laser treated over 5 mm \times 5 mm areas with the aid of a fully automated laser micromachining workstation incorporating a Spectra-Physics Pulseo[®] 355-20 DPSS laser (Spectra-Physics, Santa Clara, CA, USA) with average power in excess of 20 W at $\lambda=355$ nm and 100 kHz repetition rate at UPM Laser Centre (Figure 1).

The laser beam was guided over the sample surface by an optical system that included six mirrors, a beam expander, a digital scanner, and a lens with 250 mm focal length. The experiments were performed at fixed pulse duration of about 30 ns. The laser beam has Gaussian power density profile, and the machining was performed in atmospheric conditions with an apparent spot size of 15 μm . Two sets of samples were produced at a power 300 mW, with the geometry



Figure 1: Experimental workstation equipped with ns pulse UV DPSS laser used for the reported experiments at UPM Laser Centre.

of microchannels and micropillars. The microchannels and micropillars are separated by distance in the range of 10–25 μm . The distance is, hereafter, termed as pitch ‘P’ for future reference in the text. The detailed laser processing conditions are listed in Table 1.

The laser-machined surface patterns were analyzed with scanning electron microscope (SEM) equipped with energy-dispersive X-ray spectroscopy (HITACHI, Model S-3000N[®], Hitachi Corporation, Japan) and confocal laser scanning microscope (CLSM, LEICA DCM 3D[®], Leitz Corporation, Wetzlar, Germany) to evaluate the geometry of the induced patterns. The hydrophobicity/water repellence of the samples was studied by measuring the static contact angle using the sessile drop technique, with a video-based optical contact angle measuring device (OCA 15 Plus[®] from Data Physics Instruments, Filderstadt, Germany). Eight-microliter droplets of distilled deionized water were dispensed on the laser-machined surface structures under atmospheric conditions, and the static contact angle was calculated by analyzing droplet images recorded just after the drop deposition.

3 Results and discussion

Microchannels and micropillars have been fabricated with process parameters according to Table 1. Figure 2

Table 1: Laser-processing parameters used for the generation of the described superhydrophobic patterns.

Laser power, P_L (mW)	300
Spot diameter, D (μm)	15
Fluence, F (J/cm^2)	1.6
Repetition rate, R (kHz)	100
Scan speed, v (mm/s)	40
Pitch, P (μm)	10, 15, 20, 25

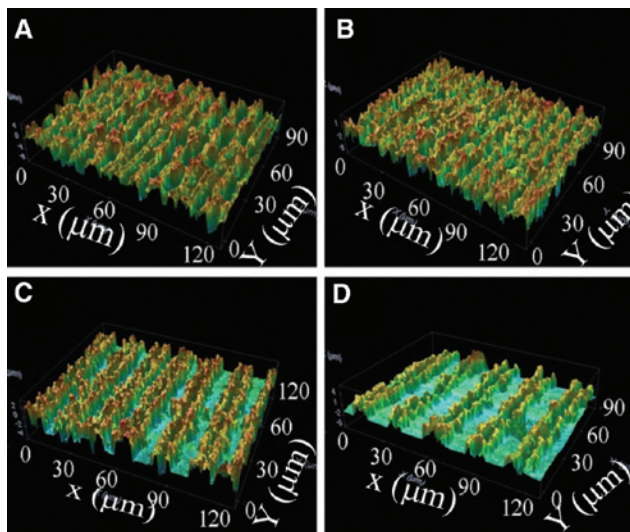


Figure 2: CLSM 3D images of the microchannels fabricated with $P_L=300$ mW, $v=40$ mm/s, and $f=100$ kHz for four different values of P: (A) 10 μm ; (B) 15 μm ; (C) 20 μm ; (D) 25 μm .

represents the CLSM 3D image of the microchannels fabricated with four values of P (10, 15, 20, and 25 μm). The widths of the respective channels were measured to be about 3, 5, 7, and 8 μm . All the microchannels recorded a depth in the range of 1.75–2.75 μm . The melt and recast formation was expected provided a nanosecond laser processing regime was used. The depth difference may be related to the fact that molten materials coming from the subsequent channels would partially fill the previously fabricated channels. Moreover, the difference in the depth could also be related to the height of the piled recast layer or micro-wall-like structure above the substrate surface, and it recorded a height of 1–2 μm with respect to the original surface. The height and width of the micro-wall is influenced by the overlap of the recast layer formed on the adjacent microchannel edges. Further, the channels fabricated by $P=10$ μm and 15 μm resulted into a near-broken state. The height of the micro-wall is influenced by melt ejection and the repeated melting of the recast by the low power density tail end of the Gaussian beam profile.

Figure 3 shows the SEM images of microchannels fabricated with a power of 300 mW. The formation of the recast layer is observed to form along the direction of the laser machining. For the sample machined with $P=10$ μm , the small horizontal shift produced very narrow microchannels, with an effective average channel width of 1.75 μm . The narrow width and reduced height can be attributed to repeated melting of the recast layer by the tail end of the Gaussian beam profile. The samples machined with $P=15$ μm , 20 μm , and 25 μm have untreated metal surface between the channels, and this allows them to have higher depths (2–2.75 μm). The improvement in the depth of the microchannels is attributed to the increase in the height of the micro-walls.

Unlike in the case of the sample treated with $P=10$ μm , the presence of spherically shaped particles on the top of the recast layer of these samples has been observed. The spherical-shaped particles are the result of the resolidification of metal vapor caused due to the ablation mechanism. Further, the aluminum surfaces have the debris spread over the unprocessed aluminum surface. The recast materials from the adjacent microchannels form an additional channel on the top surface with heights in sub-micron range. This submicron channels have been found to be advantageous with respect to the improvement of hydrophobicity of the metal surfaces.

Figure 4 shows the confocal 3D image of the micropillars fabricated with four different values of P (10, 15, 20, and 25 μm) with 300 mW laser power. The micropillars fabricated with $P=10$ μm and $P=15$ μm resulted into a scattered peak instead of peaks at regular intervals.

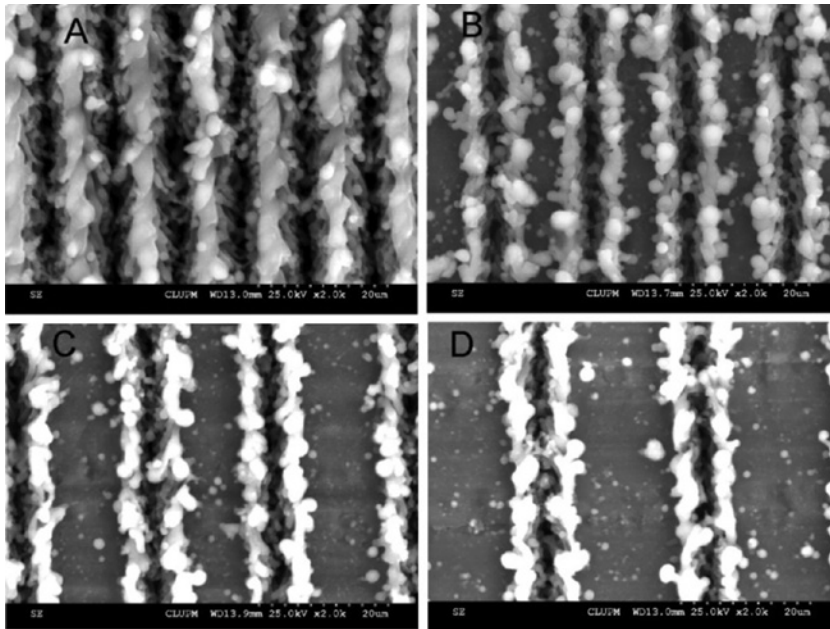


Figure 3: SEM images of the microchannels fabricated with, $P_L=300$ mW, $v=40$ mm/s, and $f=100$ kHz for four different values of P: (A) 10 μm ; (B) 15 μm ; (C) 20 μm ; (D) 25 μm .

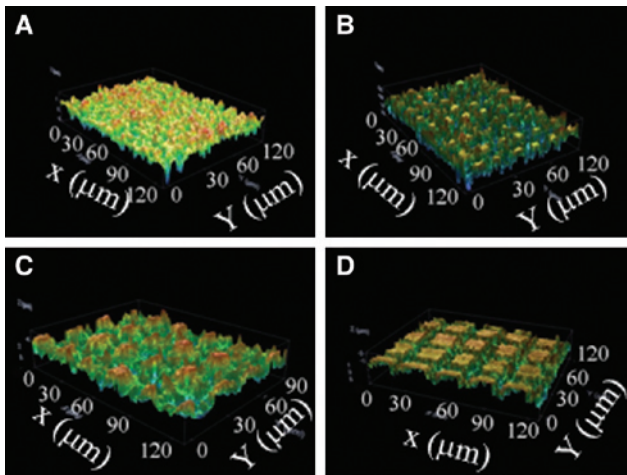


Figure 4: CLSM 3D images of the micropillars fabricated with, $P_L=300$ mW, $v=40$ mm/s, and $f=100$ kHz for four different values of P: (A) 10 μm ; (B) 15 μm ; (C) 20 μm ; (D) 25 μm .

Heavy deposition of recast material on the top surface of the micropillars is observed in these samples, whereas the micropillars fabricated with $P=20$ μm and $P=25$ μm have debris deposition over a broader circumference area. The corresponding SEM images (Figure 5) indicate the melt formation during the laser ablation. It is clear that the molten material solidifies along the direction of the laser motion. For all the four values of P, the channels are opened in one direction and closed on the perpendicular direction. This is caused by the ejection of the melt formed during

the laser processing. In addition to the heavy piling up of recast material on the top edges of micropillars, spherical-shaped resolidified metal vapor structures are also found. This may be the self-cooled metal vapor from the plasma generated by laser ablation.

In this kind of structures, the piling of the recast is observed to form a μ -cell or closed-packet-like structure on the top of the micropillars as shown in Figure 6. In this case, the μ -cell structure is separated by 10- to 15- μm channels. Therefore, the laser-patterned aluminum surface has two different patterns such as micropillars and μ -cells, thus, reducing the fraction of solid area in contact with the water droplets. This fact provides an important advantage where water repellence is concerned. The closed microchannels act as micro packets and can hold small volumes of air trapped inside the pockets that, in turn, can be used to prevent the water to flush out the air inside the narrow microchannels.

The effect of the generated micropatterns on the wetting properties of the Al samples was evaluated by static sessile drop contact angle measurements, using a droplet size of 8 μl . The plain Al surface recorded a SCA value of $85\pm 3^\circ$. The entire laser-patterned surface was highly hydrophilic within minutes of processing. The SCA measurements were performed after 24 h and after different successive time periods and invariably exhibited the hydrophobic character that provides a strong argument about the stability of the generated structures. The SCA measurements show an increase in SCA values with

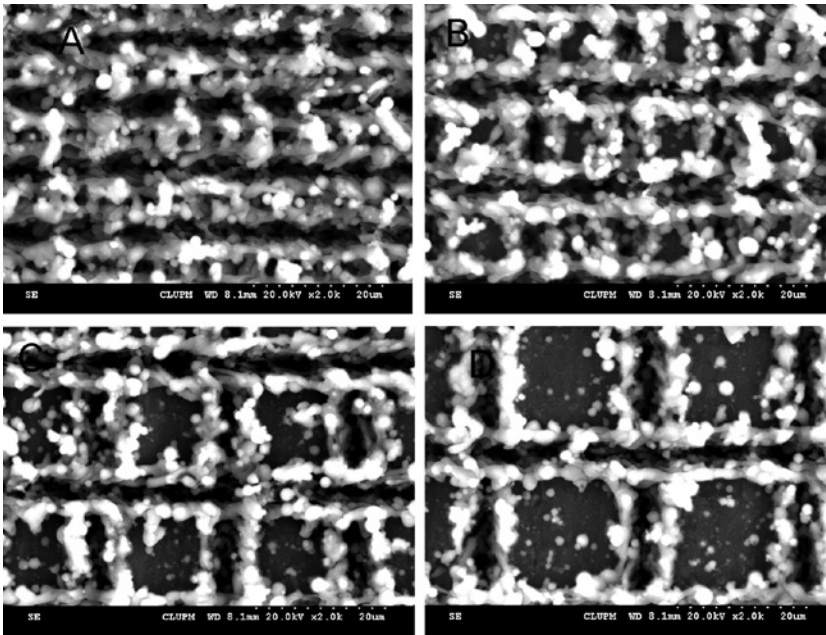


Figure 5: SEM image of the micropillars fabricated with, $P_L=300$ mW, $v=40$ mm/s, and $f=100$ kHz for four different values of P: (A) 10 μm ; (B) 15 μm ; (C) 20 μm ; (D) 25 μm .

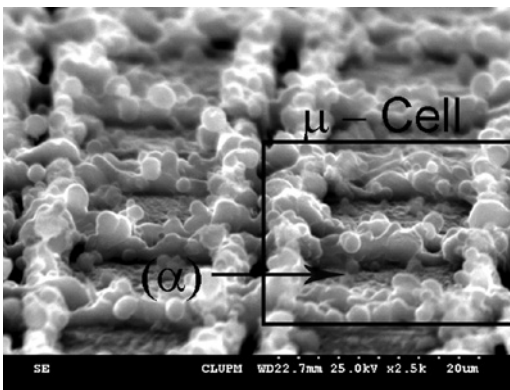


Figure 6: SEM image of μ -cell formation on top of the micropillars ($P=25$ μm).

respect to P and starts declination beyond $P=20$ μm for micropillar structures, as shown in Figure 7. The SCA measurements on the microchannel patterns show a similar trend as the micropillars, and it saturates as the P is increased beyond 20 μm . For the cases where the water droplets are unable to dispense or land on the surface from the microsyringe, the normal sessile droplet technique is not applicable. The SCA of this kind of surface is considered to be 180° (see, i.e. ref. [16]) or ultrahydrophobic surface. The low values of SCA for the sample processed with $P=15$ μm may be due to the lack of formation of the μ -cell structure. Samples with micropillar geometry exhibited ultrahydrophobicity for the samples processed

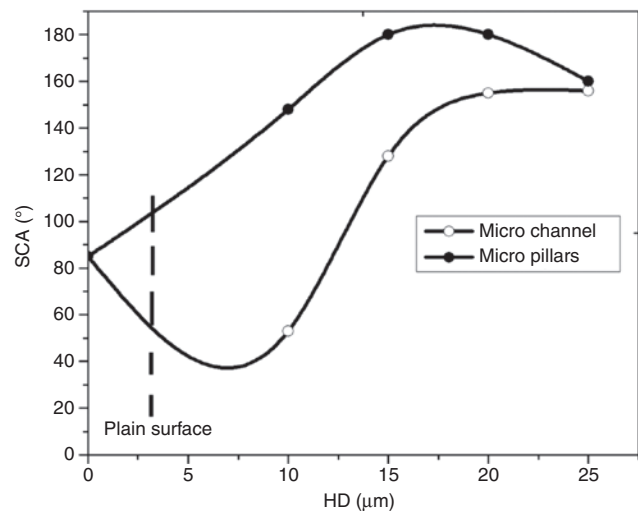


Figure 7: Static contact angle for the microchannels and micropillars as a function hatch distance.

with $P=15$ μm and 20 μm . The sample processed $P=25$ μm recorded a SCA of 160° . When the droplet is dispensed on the laser patterned surface, the water droplet has contact only with the top edge of the μ -walls due to the small volume of air trapped in the μ -cell structures. The air bubbles act as cushion for the water droplet, thus, avoiding the contact with the bottom surface of the μ -cell structures. The contact line composed of solid-liquid-air has been explained by the Cassie-Baxter model [20].

The ultrahydrophobicity of the generated micropatterns may be clearly attributed to the formation of μ -cell structure on the top of the micropillars. However, the micropillar geometry recorded a decline in the SCA values as the P is increased from 20 μm . This reduction may be due to the increase in spacing between the μ -cell structures, which would confirm the proposed hypothesis. When a water droplet is dispensed on the surface, it wets the hydrophilic surface (which is marked as (α) on the top of the micropillar, Figure 6) and dewets the ultrahydrophobic μ walls. Therefore, when the P is increased, the water is exposed to the larger hydrophilic surface (α) and tends to land on the surface resulting in a SCA of 160° .

4 Conclusions

In the present study, the application of nanosecond laser pulses on the flat surfaces of aluminum (Al) in a one-step process leading to the generation of extended areas of stable superhydrophobic behavior has been discussed. Both laser-generated periodic structures consisting in laser channels and laser pillars have been successfully developed with the aid of a 30-ns pulse, 100-kHz repetition rate, and 300-mW average power laser emitting at $\lambda=355$ nm working at a selected focus diameter and scan speed for different hatch distance values. The resulting micropatterns were evaluated by scanning electron microscopy (SEM) and confocal laser scanning microscopy (CLSM) in order to make apparent the material/geometrical parameters of the generated structures, and a direct measurement of the static contact angle (SCA) was performed in order to evaluate the wettability of the generated surface.

Among other interesting conclusions referring to the long-term stability of the generated patterns (mostly as a consequence of the intimate integration of recast into base material), a conceptually relevant methodology has been defined for the systematic generation of hierarchical-like micro/nano-structures fulfilling the conditions for the generation of superhydrophobic surfaces through the generation of μ -cells able to serve as air-trapping structures responsible for a substantially inhibited wettability of the substrate.

This development, clearly deserving further deeper studies in its road to industrial implementation, is now considered as the basis for the systematic single-step generation of large-scale extended surfaces with adjusted wettability properties as required by the different kinds of self-cleaning applications. Undoubtedly, the demonstrated possibility of use of ns lasers with their present-day

industrial robustness and their amenability to processing workstations with high-throughput properties will contribute to the industrial implementation of the described developments.

Acknowledgments: The authors are thankful to BSH Electrodomésticos España S.A. for their support in executing this work.

References

- [1] X. Yao, Y. Song, and L. Jiang, *Adv. Mater.* 23, 719–734 (2011).
- [2] T. L. Sun and G. Y. Qing, *Adv. Mater.* 23, H57–H77 (2011).
- [3] R. Jagdheesh, *Langmuir* 30, 12067–12073 (2014).
- [4] R. Jagdheesh, B. Pathiraj, E. Karatay, G. R. B. E. Romer and A. J. Huis in't Veld, *Langmuir* 27, 8464–8469 (2011).
- [5] S. Wolff and I. Saxena, *Manuf. Lett.* 2, 54–59 (2014).
- [6] S. Torres-Peiró, J. González-Ausejo, O. Mendoza-Yero, G. Mínguez-Vega and J. Lancis, *Appl. Surf. Sci.* 303, 393–398 (2014).
- [7] B. N. Chichkov, C. Momma, S. Nolte, F. von Alvensleben and A. Tünnermann, *Appl. Phys. A* 63, 109–115 (1996).
- [8] D. Breitling, A. Ruf, and F. Dausinger, in 'Proc. SPIE 5339, Photon Processing in Microelectronics and Photonics III, 49 (July 15, 2004)'; doi:10.1117/12.541434; <http://dx.doi.org/10.1117/12.541434>.
- [9] K.-H. Leitz, B. Redlingshöfer, Y. Reg, A. Otto and M. Schmidt, *Physics Procedia* 12, 230–238 (2011).
- [10] C. Molpeceres, S. Lauzurica, J. J. García-Ballesteros, M. Morales and J. L. Ocaña, *Microelectron. Eng.* 84, 1337–1340 (2007).
- [11] M. R. H. Knowles, G. Rutterford, D. Karnakis and A. Ferguson, *Int. J. Adv. Manuf. Technol.* 33, 95–102 (2007).
- [12] T. Jiang, J. Koch, C. Unger, E. Fadeeva, A. Koroleva, et al., *Appl. Phys. A* 108, 863–869 (2012).
- [13] A.-M. Kietzig, G. Savvas, P. Hatzikiriakos and P. Englezos, *Langmuir* 25, 4821–4827 (2009).
- [14] J. P. Ulerich, L. C. Ionescu, J. Chen, W. O. Soboyejo and C. B. Arnold, in 'Photon Processing in Microelectronics and Photonics VI', Ed. by C. B. Arnold, T. Okada, M. Meunier, A. S. Holmes, D. B. Geohegan, F. Träger and J. J. Dubowski, *Proc. of SPIE* 6458, 645819 (2007) 0277-786X/07/\$18, doi: 10.1117/12.713964.
- [15] S. Mukherjee, in 'Proceedings of the 1st International Electronic Conference on Materials'; 05/2014. Available at <http://sciforum.net/conference/ecm-1>.
- [16] J. Long, M. Zhong, H. Zhang and P. Fan, *J. Colloid Interface Sci.* 441, 1–9 (2015).
- [17] A. Y. Vorobyev and G. Chunlei, *J. Appl. Phys.* 117, 033103–033105 (2015).
- [18] L. Torrisi and C. Scolaro, *Acta Physica Polonica A* 128, 48–53 (2015).
- [19] M. V. Rukosuyev, J. Lee, Seong, J. Cho, G. Lim, et al., *Appl. Surf. Sci.* 313, 411–417 (2014).
- [20] A. B. D. Cassie and S. Baxter, *Trans. Faraday Soc.* 40, 546–551 (1944).



Jose L. Ocaña
UPM Laser Centre, Universidad Politécnica
de Madrid, Ctra. Valencia, km 7.3, 28031
Madrid, Spain
jlocana@etsii.upm.es

Jose L. Ocaña was awarded his MSc (1979) and a PhD (1982) in Industrial Engineering (Energy) at the Polytechnical University of Madrid (Spain). He is Chair Professor of Mechanical Engineering at the ETSII-UPM School of Engineering and Director of the UPM Laser Centre at this University. He is responsible for coordination of worldwide R&D initiatives in the field of scientific and industrial applications of high-power lasers, especially in high-intensity laser-matter interaction, laser welding, laser surface treatments, laser micromachining, and on-line monitoring and control of industrial laser applications. Author/coauthor of more than 150 scientific papers and more than 200 communications in the field of laser technology and applications. Former Chairman of EULASNET II (Eureka Umbrella Network for Laser Technology and Applications). Member of the Executive Board of the European Laser Institute (ELI).



J.J. García-Ballesteros
UPM Laser Centre, Universidad Politécnica
de Madrid, 28031 Madrid, Spain

J.J. García-Ballesteros, was awarded his MSc in Physics (2004) and PhD in Applied Sciences (2016) at the Polytechnical University of Madrid (Spain). Specialist in short pulse laser-matter interaction and development of laser micromanufacturing applications, with high experience in ns and ps laser systems.



R. Jagdheesh
UPM Laser Centre, Universidad Politécnica
de Madrid, 28031 Madrid, Spain

R. Jagdheesh, was awarded his MSc (1998) and PhD (2005) in Physics from Bharathidasan University, India. After the PhD, he worked as postdoctoral fellow at Raja Ramanna Centre for Advanced Technologies in India, ENSMA CNRS in France, University of Twente in Netherlands, and University of New South Wales, Australia before he joined the CLUPM, Polytechnical University of Madrid in Spain. His research is focused on laser cladding, laser surface alloying and laser micromachining for surface functionalization. He has published more than 35 research papers in journals and conference proceedings.